1 x 5 MEMS Mode Selective Switch with an Inverse-Designed Silicon Nitride MDM

Julian L. Pita Ruiz, Almur A. S. Rabih, Seyedfakhreddin Nabavi, Frederic Nabki, and Michaël Ménard

Department of Electrical Engineering, École de Technologie Supérieure (ÉTS), Montreal, QC, H3C 1K3, Canada

julian-leonel.pita-ruiz@etsmtl.ca

Abstract: We present the first experimental demonstration of an inverse-designed 5-mode division multiplexer (MDM) in silicon nitride for MEMS-based inter-chip switches. The MDM exhibits high efficiency, wide bandwidth, compactness, robust fabrication, and compatibility with commercial foundry production.

1. Introduction

While well-established silicon platforms are highly versatile, they alone cannot meet the growing demand for high-speed optical communications [1, 2]. Consequently, significant breakthroughs in the integration of various materials have occurred over the past decade, enabling the packaging of diverse photonic integrated circuits (PICs) with enhanced functionalities that were previously unattainable using a single-platform PIC [3, 4]. However, this integration presents substantial challenges, particularly in implementing efficient interconnects between different PICs, primarily due to the complexity of achieving sub-micron alignment [5–7].

We present a proof-of-concept for a 5-mode inter-chip switch using an electrothermal micro-electromechanical systems (MEMS) positioner and a mode-division multiplexer (MDM). The MEMS micropositioner achieves both lateral and longitudinal displacements of a silicon nitride waveguide of over 6 µm, while the ultra-compact MDM requires a lateral displacement of only 4.8 µm to cover 5 channels. This enables the creation of a switch with a significantly higher number of output ports than is possible with single-mode waveguides, since the distance between single-mode waveguides must be large enough to avoid crosstalk. We fabricated and measured an MDM with 5 different input waveguide positions, all positioned with a residual gap of 345 nm to emulate the presence of a MEMS positioner. The device exhibited remarkable performance, with the maximum average transmission being -1.46 dB for the TE_{00} mode, while all other modes maintained values above -1.85 dB. Additionally, the minimum measured crosstalk (XT) of -16.7 dB was for TE_{40} mode, and the 3-dB bandwidth for all modes covers the entire C and L communication bands.

2. Design

The platform used to design the MEMS positioner is based on the devices demonstrated in [5–7] and consists of an optical stack with two 3.4 µm silicon dioxide cladding layers and a 435 nm silicon nitride layer. It also includes a silicon-on-insulator (SOI) stack with a prefabricated MEMS cavity. This SOI stack consists of a 59 µm silicon layer, a 1 µm buried silicon oxide layer, and a 725 µm silicon substrate. In addition, an AlCu layer is used on electrical pads for MEMS actuation. A cross-section view of this platform is shown in Figure 1a.

Figure 1b shows a schematic of the MEMS positioner with a suspended platform holding an 850 nm wide movable silicon nitride waveguide. This waveguide can be precisely positioned at the required locations on the fixed MDM in chip A, achieving submicron precision. Lateral and longitudinal displacements are provided by three electrothermal chevron actuators. The longitudinal (i.e., gap closing) actuator moves the platform toward chip A to bring the movable waveguide into close proximity with the MDM. Moreover, the lateral actuators allow the selection of the desired mode of the multimode waveguide to which the input signal is coupled, as shown in the inset of Figure 1b, where the black rectangles indicate the positions of the movable waveguide. It is worth noting that a smaller gap results in a higher transmission for each mode. Figure 1c shows the simulated lateral and longitudinal displacements of the movable waveguide as a function of actuation voltage. A lateral displacement of 6 µm is achieved with an actuation voltage of 14 V, while the 2.4 µm displacement required to select between the 5 modes of the multimode waveguide is achieved with less than 11 V. In addition, a longitudinal displacement of 6 µm is achieved with a voltage of 17 V, allowing chips A and B to be positioned at least 6 µm apart. Figure 1d shows the excited modes in the multimode waveguide of chip A, along with their corresponding excitation positional mode at the input of the MDM.

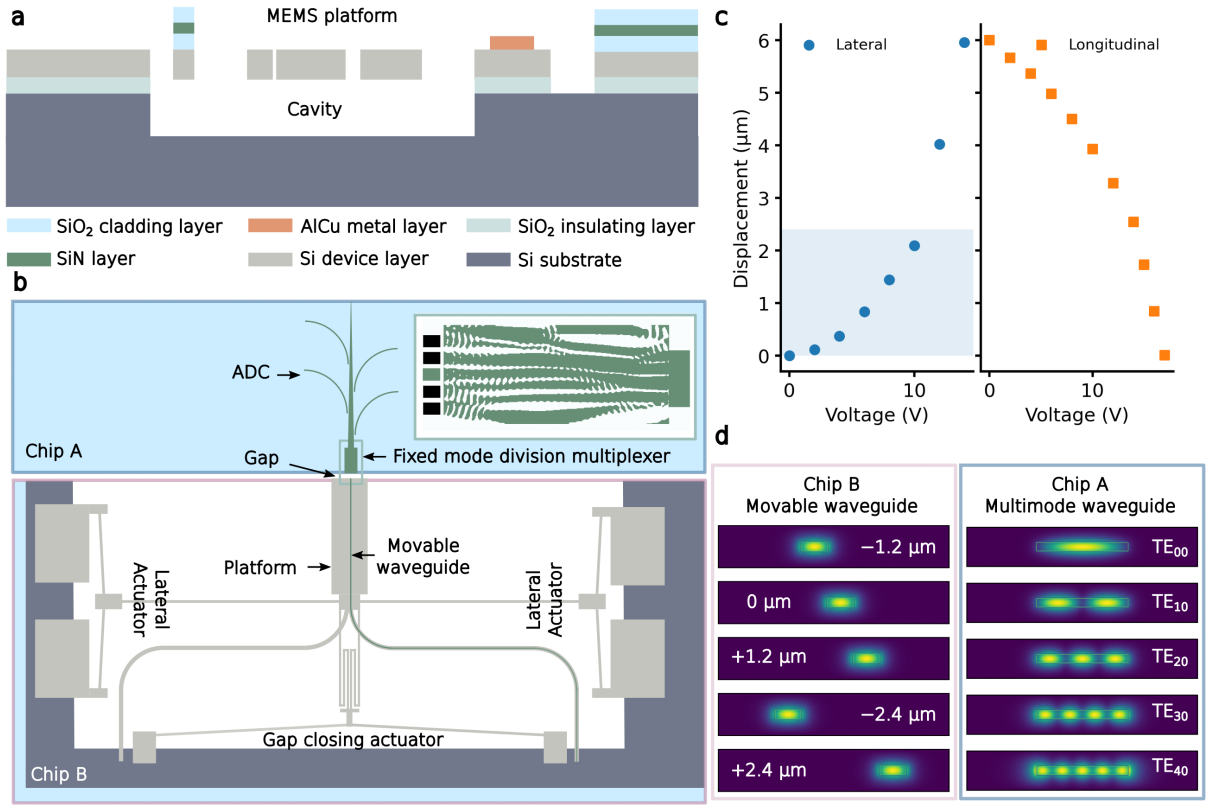

Fig. 1: **Silicon Nitride Inter-Chip Mode Selecting Switch.** a) Cross-section view of the platform used to design the two-axis MEMS micropositioner compatible with the fabrication process of AEPONYX Inc. b) Schematic of the two chips used for the mode-selecting switch. Chip A shows the inverse-designed MDM and an asymmetric directional coupler mode demultiplexer. An inset of this first structure is included, showing the different positions of the input waveguide. Chip B shows the electrothermal MEMS waveguide micropositioner. c) Simulated lateral and longitudinal displacements. The former is symmetrical on both sides, and the faint blue stripe indicates the displacement necessary to excite the 5 modes. d) The electric field of the moving input waveguides in chip B and the electric field in chip A of the excited high-order modes corresponding to each waveguide position in chip B.

3. Results

Several MDMs were fabricated by ANT to replicate the 5 input positions of the movable waveguide on Chip B. Fixed waveguides, measuring 850 nm × 435 nm, were positioned at 345 nm from the MDM to emulate the gap between the two chips after actuating the MEMS. To optimize the MDM, LumOpt in Lumerical was employed, aiming to maximize the coupling efficiency between each of the 5 positions of the single-mode movable waveguide and the initial 5 TE modes of the 4 µm × 400 nm multimode output waveguide. Despite the minimum feature size of 120 nm allowed by the fabrication process, we opted for 160 nm to enhance the device robustness during manufacturing. Additionally, a series of simulations were conducted to define the optimal device size, the effective displacement distance of the movable waveguide, and which waveguide position at the input excited which specific mode at the multimode output. This effort resulted in a device with a footprint of 16 µm × 7 µm and a pitch between modal channels of the movable waveguide set at 1.2 µm. In Figure 2a, a top-view of the electric field distribution of the MDM is depicted for each of the 5 input positions of the movable waveguide. It is readily apparent that each position generates a field distribution that distinctly couples to a different mode of the multimode waveguide, signifying high transmission efficiency. Figure 2b provides further confirmation of the high coupling efficiency of the device with a maximum simulated average transmission exceeding −1.49 dB for all modes. The figure also shows a 3-dB bandwidth that extends beyond the C and L communication bands, and modal crosstalk exhibits a maximum of −13 dB for the TE_{10} mode and a minimum of −16.7 dB for the TE_{40} mode. Figure 2c displays scanning electron microscopy (SEM) images of the MDM with different input waveguide configurations, showing a close correspondence to the refractive index distribution obtained from the optimization, as observed in the inset of Figure 1b. Finally, in Figure 2d, the performance of the fabricated device is presented, revealing an average transmission of −1.46 dB for TE_{00} mode, −1.53 dB for TE_{10} mode, −1.56 dB for TE_{20} mode, −1.85 dB for TE_{30} mode, and −1.50 dB for TE_{40} mode. The maximum modal crosstalk consistently remains below −12 dB and reaches −16.7 dB for TE_{40} mode. The 3-dB bandwidth matches the simulation results and surpasses 95 nm.

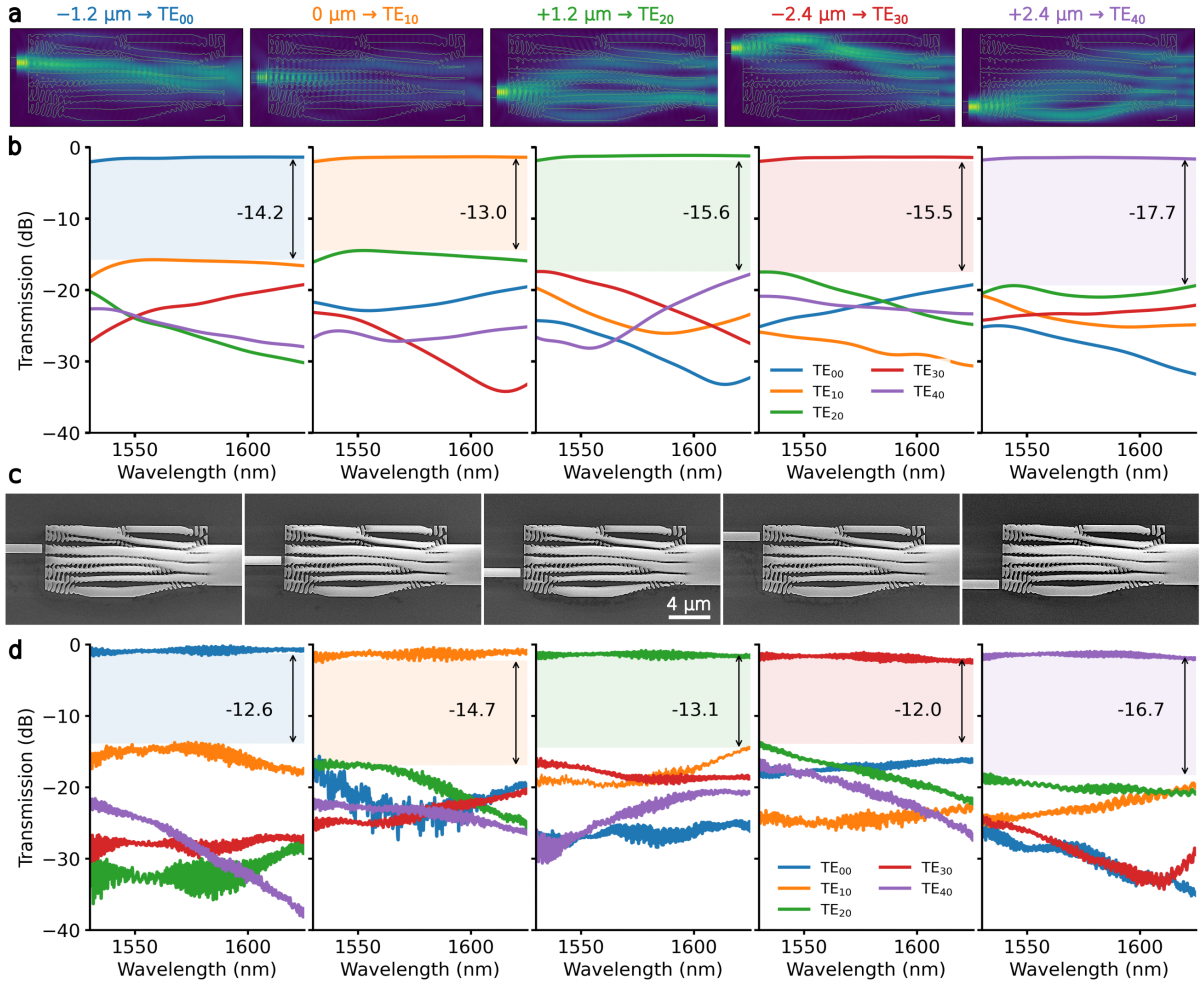

Fig. 2: **Performance of the MDM**. a) Electric field superimposed over the contour of the mode-divisor multiplexer structure and the movable input waveguide. b) Simulated transmission and crosstalk across the entire C and L communication bands for each waveguide position. The colored stripes indicate the maximum crosstalk for each high-order mode in the simulated band. c) SEM images of the MDM with different positions of the input waveguide. d) Measured transmission and crosstalk across the entire C and L communication bands for each waveguide position. Similarly to b), the colored bands indicate the maximum crosstalk measured.

In conclusion, we successfully demonstrated a high-efficiency and wide-bandwidth MDM for integration with MEMS micropositioning devices. This union not only establishes high-performance interconnections between different PICs within a single package but also serves as a versatile multimode switch between two PICs.

Acknowledgments. The authors thank AEPONYX Inc. and CMC Microsystems for their support.

References

1. R. Blum, "Integrated silicon photonics for high-volume data center applications," Opt. Interconnects XX **11286**, 141–149 (2020).
2. T. Komljenovic, D. Huang, P. Pintus, M. A. Tran, M. L. Davenport, and J. E. Bowers, "Photonic integrated circuits using heterogeneous integration on silicon," Proc. IEEE **106**, 2246–2257 (2018).
3. R. Baets, A. Z. Subramanian, S. Clemmen, B. Kuyken, P. Bienstman, N. Le Thomas, G. Roelkens, D. Van Thourhout, P. Helin, and S. Severi, "Silicon photonics: Silicon nitride versus silicon-on-insulator," in *Optical Fiber Communication Conference,* (Optica Publishing Group, 2016), pp. Th3J–1.
4. P. Kaur, A. Boes, G. Ren, T. G. Nguyen, G. Roelkens, and A. Mitchell, "Hybrid and heterogeneous photonic integration," APL Photonics **6** (2021).
5. S. Sharma, N. Kohli, J. Brière, F. Nabki, and M. Ménard, "Integrated 1× 3 mems silicon nitride photonics switch," Opt. Express **30**, 22200–22220 (2022).
6. A. A. Rabih, S. Sharma, J. Pita, M. Ménard, and F. Nabki, "Two-axis mems positioner for waveguide alignment in silicon nitride photonic integrated circuits," Opt. Express **31**, 30797–30814 (2023).
7. B. Barazani, A. Gascon, C. Coia, F. Nabki, and M. Ménard, "Broadband 1 x 4 silicon nitride photonic switch fabricated on a hybrid electrothermal and electrostatic mems platform," J. Light. Technol. (2023).